Engineering Science
2023; 8(1): 6-13
http://www.sciencepublishinggroup.com/j/es
doi: 10.11648/j.es.20230801.12
ISSN: 2578-9260 (Print); ISSN: 2578-9279 (Online)

Design and Mechanical Characteristics Analysis of Deep Sea Manifold System

Chuxiang Lin†, Weili Wang†, Yongmei Zhu*, Jian Zhang*, Suzhou Zhang, Longhui Wang

School of Mechanical Engineering, Jiangsu University of Science and Technology, Zhenjiang, China

Email address:

linasuka103@163.com (Chuxiang Lin), zymtt@163.com (Yongmei Zhu), 18296158303@163.com (Weili Wang), zhjian127@163.com (Jian Zhang), 2027840641 @qq.com (Suzhou Zhang), w2873848298@163.com (Longhui Wang)

*Corresponding author

† Chuxiang Lin and Weili Wang are co-first author

To cite this article:

Chuxiang Lin, Weili Wang, Yongmei Zhu, Jian Zhang, Suzhou Zhang, Longhui Wang. Design and Mechanical Characteristics Analysis of Deep Sea Manifold System. *Engineering Science*. Vol. 8, No. 1, 2023, pp. 6-13. doi: 10.11648/j.es.20230801.12

Received: April 6, 2023; **Accepted**: April 24, 2023; **Published**: May 10, 2023

Abstract: Subsea manifolds are important equipment for offshore oil and gas extraction. The layout of the manifold is related to both the difficulty of fabrication and the installation and maintenance of the manifold. Based on 1500 m deep sea conditions and 68.9 MPa pipeline fluid pressure, the overall design of a double well groove and double collector subsea manifold is investigated, the selection of specific parameters is discussed in detail. The arrangement of different valves and pipelines and the efficiency of space volume usage are discussed. Stress analysis of the designed manifold as a whole was carried out using AutoPIPE software and its strength was assessed according to the applicable American Society of Mechanical Engineers (ASME) standards. It was found that the maximum stress ratio was 0.9 for radial stresses and relatively small for axial stresses, but both met the design requirements for deep sea manifold piping. Finally, linear and nonlinear buckling analyses of circular arc pipes were carried out, the fifth-order linear eigenvalue buckling modes, linear critical buckling load and nonlinear critical buckling load were obtained. It is found that the nonlinear critical buckling load was 20.5% lower than the linear critical buckling load. The failure mode of post-buckling is local dimple, which is located at the initial defect, indicating that early geometric defects have a greater influence on the load carrying limit of the pipe. This paper can provide a reference for the study of common technologies for the design of deepwater subsea pipeline manifolds and subsea production facilities.

Keywords: Manifold System, Overall Design, Strength, Stability

1. Introduction

The global consumption of oil and gas energy is increasing. Due to the continued decline of oil and gas energy in offshore and shallow waters, the extraction of oil and gas in deep sea areas has become a major challenge in the marine energy sector. As the core component of the subsea production system in deep-sea oil and gas field extraction equipment, the underwater pipe sink is mainly located near the oil tree and has the function of gathering, distributing, controlling and monitoring the flow status of oil and gas [1-3].

Several studies on underwater manifolds have been conducted in recent years by scholars and experts in relevant fields both at home and abroad. Wei et al. [4] detailed the functions and components of underwater manifolds, including manufacturing technology, construction technology, and technical difficulties. Chuan et al [5] analyzed the steel for deepwater pipe manifold structures based on the study of relevant standard codes and domestic steel for marine engineering, and summarized the domestic material standards applicable to deepwater underwater pipe manifold steel structures. Gu et al. [6] investigated the loads that underwater manifold structures can withstand under various working conditions and carried out calculation verification with SACS software, proposing a reasonable design method for deepwater manifolds. Liu [7] established a system fault tree model and conducted an agreed-upon hierarchical division of the underwater oil and

gas production system. He used the downward method to obtain the fault tree's minimum cut set and then conducted a qualitative analysis of the system. Shang et al. [8] thoroughly considered the extreme or unexpected events that may be encountered by subsea oil production facilities, and conducted qualitative and quantitative evaluations of underwater manifolds using fault tree analysis (FTA) methods. Wang et al [9] developed a complex iterative structure based on unsupervised learning methods and clustering algorithms to optimize the layout of subsea production systems. Liu et al. [10] described four types of pipeline plugging and proposed a quantitative assessment method for predicting the risk of two-way pig plugging based on the analytic hierarchy process (AHP) and the entropy combination method. Zhang et al [11] designed and calculated the arrangement scheme of the submerged pipe manifold pipeline using data from West African oil and gas fields. The cost of installing equipment makes up the majority of the total project budget in deepwater oil and gas field production costs. Reducing the overall volume and mass of the subsea manifold is critical to saving project costs and reducing the difficulty of installation, as production requirements are met and production systems are safe.

In this paper, the overall design of an underwater pipe manifold with a water depth of 1500m and a pipeline fluid pressure of 68.9MPa is studied with the operating environmental parameters of the underwater pipe manifold system in the South China Sea oil and gas field, and the setting scheme and space volume usage efficiency of different valves and pipes are presented. Stress analysis is performed on the designed pipe system using AutoPIPE software, and its strength is evaluated against the applicable American Society of Mechanical Engineers criteria. Finally, for circular arc pipes, a linear eigenvalue buckling analysis and a nonlinear buckling analysis with geometric flaws and material elastic-plasticity were performed.

2. Design of Deep-Sea Manifold System

2.1. Parameter Design of Deep Sea Pipeline

According to the specification ISO 13628-15 [12], the minimum cross-sectional area of pipe flow required to avoid fluid erosion is:

$$A = \frac{9.35 + \frac{ZRT}{21.25P}}{V_e} \tag{1}$$

Where: A is the minimum required pipe flow cross-section (in^2/1000bbl/d); V_e is the erosion velocity of the fluid (ft/s); P is the working pressure; R is the gas-to-liquid ratio under standard conditions (ft^3/bbl); T is the working temperature (°R); Z is the gas compression coefficient. According to the wellhead parameters of a 1.5 km deep oil and gas field, here P=4583 psi, Z=0.91, R=2000 ft^3/bbl, T=535 °R.

According to the requirements of the specification ISO 13628-15 [12], the erosion speed is:

$$V_e = \frac{c}{\sqrt{\rho_m}} \tag{2}$$

Where: c is an empirical constant; ρ_m is the density of the gas-liquid mixture at working pressure and temperature (lb/ft^3). Here, the value of c is taken as 100.

According to the requirements of the specification ISO 13628-15 [12], The density of the gas-liquid mixture is:

$$\rho_m = \frac{12409 S_l P + 2.7 R S_g P}{198.7P + RTZ} \tag{3}$$

Where: S_l is the relative density of the liquid under standard conditions; S_g is the relative density of the gas under standard conditions. According to the physical properties of crude oil from a 1.5Km deep oil and gas field, here S_l=0.84, S_g=0.65.

To reduce interference with the separation device, a minimum velocity of approximately 10 feet per second in the two-phase flow pipe is assumed and used as a check velocity for the fluid flow in the pipe.

The required wall thickness for a particular pipe type is essentially a function of internal operating pressure and temperature. Steel pipe manufacturing standards allow wall thickness to be less than the nominal wall thickness error. For carbon steel pipes, it is generally desirable to have a corrosion/mechanical strength margin of at least 0.050 inches. If the corrosion rate can be predicted, the calculated corrosion allowance should be used.

Designed in accordance with the provisions of Section 5.3 - Pipeline Design of ISO 13628-15 [12] Underwater Structures and Manifolds, and the provisions of the Specification [13-16]:

$$t = t_{\min} + t_{corr} + t_{fab} \tag{4}$$

Where: t is the design thickness; t_{min} is the minimum calculated thickness; t_{corr} Is the pipeline corrosion allowance; t_{fab} is the manufacturing errors for pipes; The minimum calculated thickness is determined by the following formula:

$$S_k \le F_1 \delta_s T_1 \tag{5}$$

$$S_k = (P_i - P_e)\frac{D}{2t_{min}} \tag{6}$$

Where: S_k is the radial stress (MPa); δ_s is the yield strength (MPa); P_e Is the design internal pressure (bar); P_i is the hydrostatic deep external pressure (bar); D is the nominal diameter of the pipe (mm); F_1 is the radial stress design coefficient [13]; T_1 is the temperature influence coefficient [13].

According to the applicable situation of the document [13], the corrosion allowance is taken as 4 mm in this article.

Processing and manufacturing errors are based on the allowable deviation of the normalized wall thickness. The key essential characteristic parameters of the South China Sea oil and gas field are listed in Table 1. The internal diameter and wall thickness of the pipeline are calculated. Referring to the specification [17], the nominal diameter of the header pipe was determined to be 8 inches, and the nominal diameter of the branch pipe was determined to be 6 inches. The pipe material is API 5L X65, and the relevant parameters of the pipe are listed in Table 2.

Table 1. *Key basic characteristic parameters of oil and gas fields.*

water depth (km)	**1.5**
Sea water temperature (°C)	16~29 (sea surface) 3~4 (1.5 kilometers deep)
Reservoir pressure (MPa)	33-36
Reservoir temperature (°C)	105-120
working pressure (MPa)	68.9
Maximum temperature of flowing wellhead (°C)	102
Crude oil density (g/cm^3)	0.840 (20°C)

Table 2. *Pipe size and material parameters.*

Pipe type	**External diameter (mm)**	**Wall thickness (mm)**	**Materials**	**Density (kg·m3)**	**Elastic modulus (GPa)**	**Poisson's ratio**	**Yield strength (MPa)**
Header	219	34	X65	7850	210	0.3	448
Branch pipe	168	26					

2.2. Design of Deep-Sea Manifold System

The deep-sea manifold designed in this paper works in an oil and gas field with a water depth of 1500m in the South China Sea. Without considering the reservoir pressure drop, the ambient temperature is set at 0°C, the separation pressure of the reservoir is 7.5 MPa, and the reservoir pressure is 33 MPa. Figure 1 shows the layout of two typical 4-well manifolds.

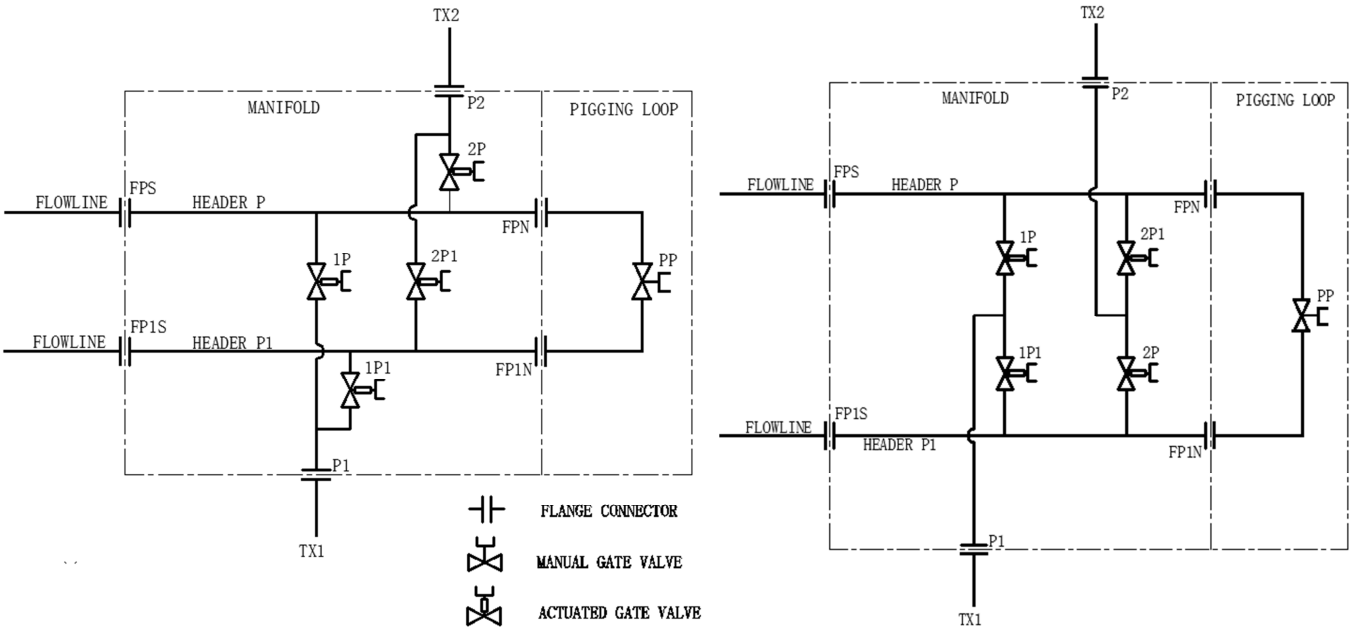

Figure 1. *Double well double header scheme. (a) Scheme A, (b) Scheme B.*

From the analysis, it can be seen that four valves in Scheme A are set between two mains, two valves in Scheme B are set between two mains, and the other two are set on both sides of the mains. It can be seen from the observation that the valve settings in Scheme A is relatively centralized compared to Scheme B. The center of gravity of the pipe manifold in Scheme A is also at a smaller distance from its geometric center, which facilitates offshore lifting and high space utilization. Therefore, from the perspective of space utilization, Scheme A is superior to Scheme B.

When selecting pipe fittings, the specification indicates a minimum radius of curvature of 3D for a header with a

clearing function, so the minimum distance between two connected header pipes is 6D. In actual design, the location of the connection of the reserved branch pipes and the mounting dimensions of the valves and sensors will also be considered. Referring to the specification ISO 13628-15 [12], this paper proposes A and B layout scheme with double groove wells as the minimum units. The specific parameters are listed in Table 3.

Table 3. *Parameters of the double well and double head Schemes.*

Schemes	Manifold size (mm × mm × mm)	Manifold quality (kg)
A	420 × 280 × 160	10000
B	500× 360 × 160	12000

Taking into account many factors such as the mounting space of the connecting device and the accuracy of the ROV robot, the smaller and lighter Scheme A has been chosen for this paper.

Because the increase in volume leads to a thicker structure is the main reason for the increase in sink mass. And in the case of the multi-well slotted sink, because the use of multiple minimum units will cause the minimum unit size chain to be superimposed, increasing the unnecessary size. Based on the above analysis, the sink structure was modeled for the valve arrangement of scenario a, as shown in Figure 2:

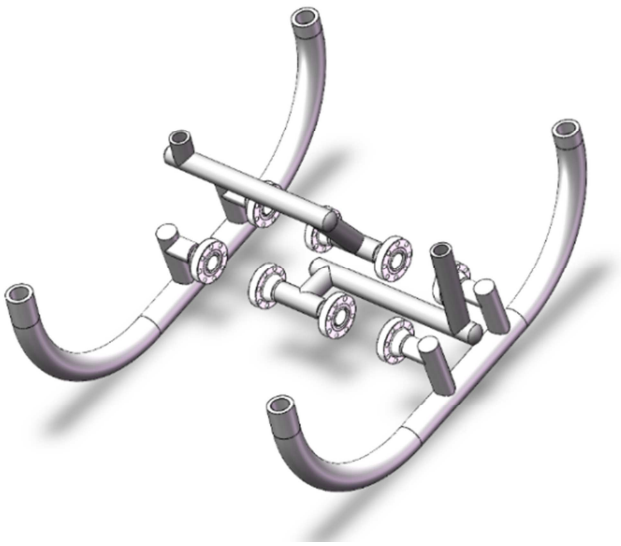

Figure 2. *Pipeline structure model.*

3. Strength Calculation of Deep Sea Pipelines

The stress conditions in the pipeline determine the reliability of the entire system. Complex piping systems will be subjected not only to internal and external pressures on the piping, but also to certain bending moments and torques due to their weight, loads applied by the cross-pipe and deformations caused by the working temperature.

(1) Radial stress

The radial stress calculation formula is shown in Equations (5) and (6).

(2) Axial stress

The axial stress criterion for pipes is:

$$\left|S_L\right| = Max[S_a + S_b, S_a - S_b] \le F_2 \cdot \delta_s \tag{7}$$

$$S_a = F_a / A \tag{8}$$

$$S_b = \pm\sqrt{\left(i_i M_i\right)^2 + \left(i_a M_a\right)^2} / Z \tag{9}$$

Where: S_L is the maximum axial stress (MPa); S_a is the axial stress (MPa); S_b is the maximum comprehensive bending stress (MPa); F_2 is the axial stress design coefficient [18]; δ_s is the yield strength (MPa); F_a is the axial force (N); A is the cross-sectional area of the pipe (mm^2); i_i is the in-plane stress enhancement coefficient [18]; M_i is the in-plane bending moment (N·m); M_a is the out-of-plane bending moment (N·m); i_a is the out-of-plane stress enhancement coefficient [18]; Z is the pipeline interface modulus (cm^3).

(3) Combined stress

There are two checking formulas for combined stress, one is the maximum shear stress formula (Tresca combined stress); The other is the maximum failure energy theory (Von Mises combined stress). The equation for the combined Tresca stress is:

$$2\left[\sqrt{\left(\frac{S_L - S_k}{2}\right)^2 + S_t^2}\right] \le F_3 \cdot \delta_s \tag{10}$$

$$S_t = M_t / 2Z \tag{11}$$

Where: S_t is torsional stress (MPa); M_t is torque (N·m); F_3 is the combined stress design factor [18].

Von Mises The combined stress calculation formula is:

$$\sqrt{S_k^2 - S_L S_k + S_L^2 + 3S_t^2} \le F_3 \cdot \delta_s \tag{12}$$

This article uses AutoPIPE software to perform stress analysis on the manifold. The nominal diameter f of the header and branch pipes is 8 inches and 6 inches respectively, with a thickness of 34 mm and 26 mm. The pipeline pressure is set at 68.9 MPa, the material is API 5L X65, the ambient temperature is 0 ° C, and the weight of a single gate valve is 1500 kg. Due to the fixed connection between the header and branch interfaces and the overall structure of the manifold, fully constrained boundary conditions were used. The calculated combined stresses are shown in Figure 3. The maximum values of circumferential, longitudinal, and combined stresses are shown in Table 4. Under this working condition, the maximum calculated combined stress at the header connection is 351.2 MPa and the allowable combined stress is 403.3 MPa, with a stress ratio of 87%.

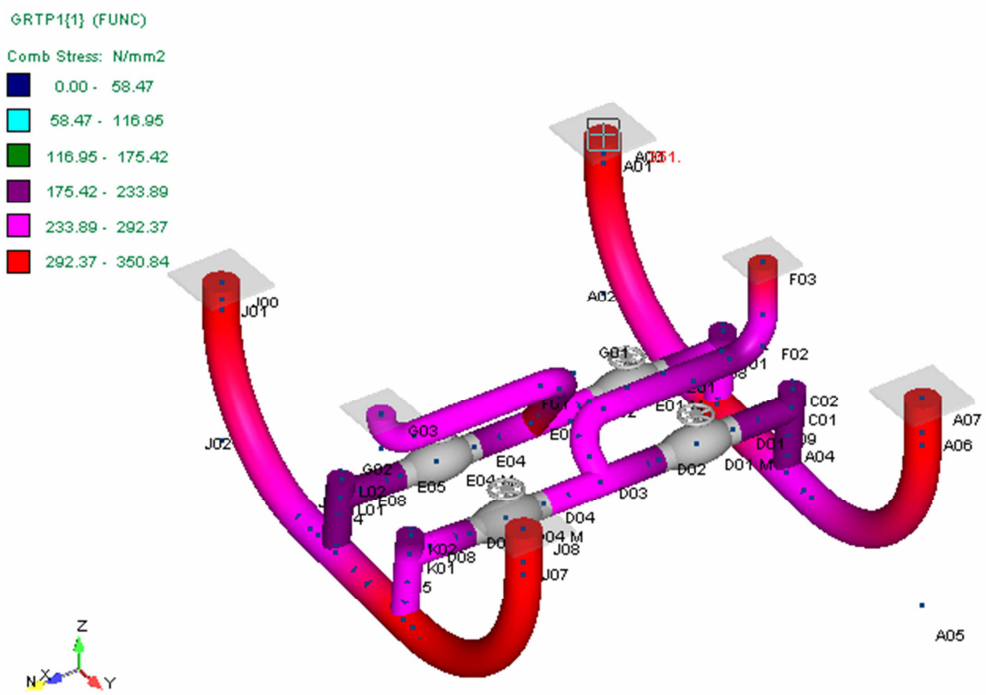

Figure 3. *Results of the manifold combination stress analysis.*

Table 4. *Results of three types of stress calculations.*

Type	Maximum stress (MPa)	Allowable stress (MPa)	Maximum stress ratio
Radial stress	201	224.1	0.9
Axial stress	163.8	358.5	0.46
Combined stress	351.2	403.3	0.87

The results indicated that the structure and parameters designed in this paper meet the specification requirements and satisfy the design requirements of the deep-sea pipe manifold pipeline.

4. Stability Analysis of Deep Sea Pipeline

Submarine pipelines may be subjected to multiple loads simultaneously during laying and service, and the torque generated during the laying process may have a certain impact on pipeline buckling [19]. When a pipeline undergoes global buckling, it will undergo significant plastic deformation, even further cracking, distortion, and local buckling, which will have a significant impact on the safety of deep-sea manifolds.

Due to the fact that pipelines are prone to stress concentration and geometric defects during bending, this paper selects circular arc pipelines for stability analysis. The model diagram is shown in Figure 4, and the pipeline parameters are listed in Table 5.

Table 5. *Parameters of circular arc pipe.*

Name	Parameter
Pipe outside diameter D0 (mm)	219
Height h (mm)	267
wall thickness t (mm)	34
Bending radius R0 (mm)	1095.5
Annular tube angle α (°)	96

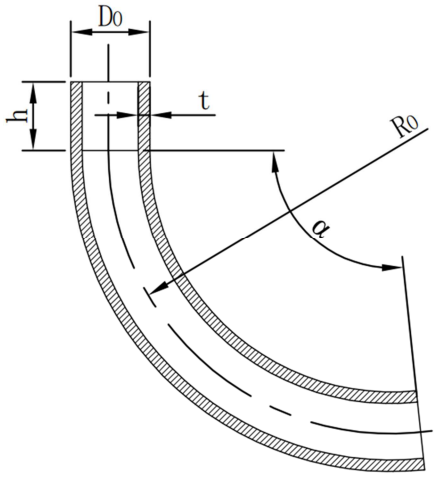

Figure 4. *Arc pipe.*

4.1. Finite Element Model

Based on the analysis and calculation of subsea pipeline conditions in actual engineering applications, the header interface is connected to the main structure of the manifold through flanges, so full fixed constraints are imposed on the upper end to limit all degrees of freedom at the upper end. When crude oil flows through the pipeline, axial displacement may occur, so the lower end releases the freedom of the liquid flow direction, as shown in Figure 5.

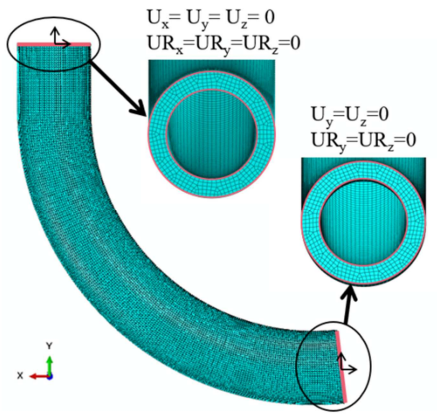

Figure 5. *Boundary conditions.*

Due to the large wall thickness of this pipe, the solid approach is used for modeling (Figure 5). The cell type is set to a three-dimensional 8-node reduced-integral cell (C3D8R). Compared with the fully integrated cell, the reduced-integral cell is faster and more accurate in calculation. However, it is worth noting that when this type of mesh is used for meshing, at least four layers of mesh are required in the thickness direction to overcome the hourglass problem. The number of cells after the above method is 87150.

For the working depth of 1500 m underwater of the pipeline, the external pressure of seawater to which the pipeline is subjected is uniformly distributed on the outer surface of the pipeline. The external load to be borne by the model is calculated according to the pressure formula specified by GL Noble Denton, and the formula is:

$$p = 0.0101 \times d \tag{13}$$

Where, p is the external pressure of seawater; d is the depth of submergence. The external ballast load on the pipeline is calculated to be about 15 MPa. The internal pressure caused by the crude oil transported by the pipeline on the inner wall of the pipeline is about 68.9 MPa.

4.2. Strength and Buckling Analysis

The pipe strength analysis results are shown in Figure 6. The results show that the maximum stress of the submarine pipeline when crude oil flows through the pipeline at 1500m underwater is 448MPa, which has reached the yield strength of the material, but only occurs at the end, and only plastic strain occurs at the end. Therefore, it is considered that the designed pipeline meets the strength requirements.

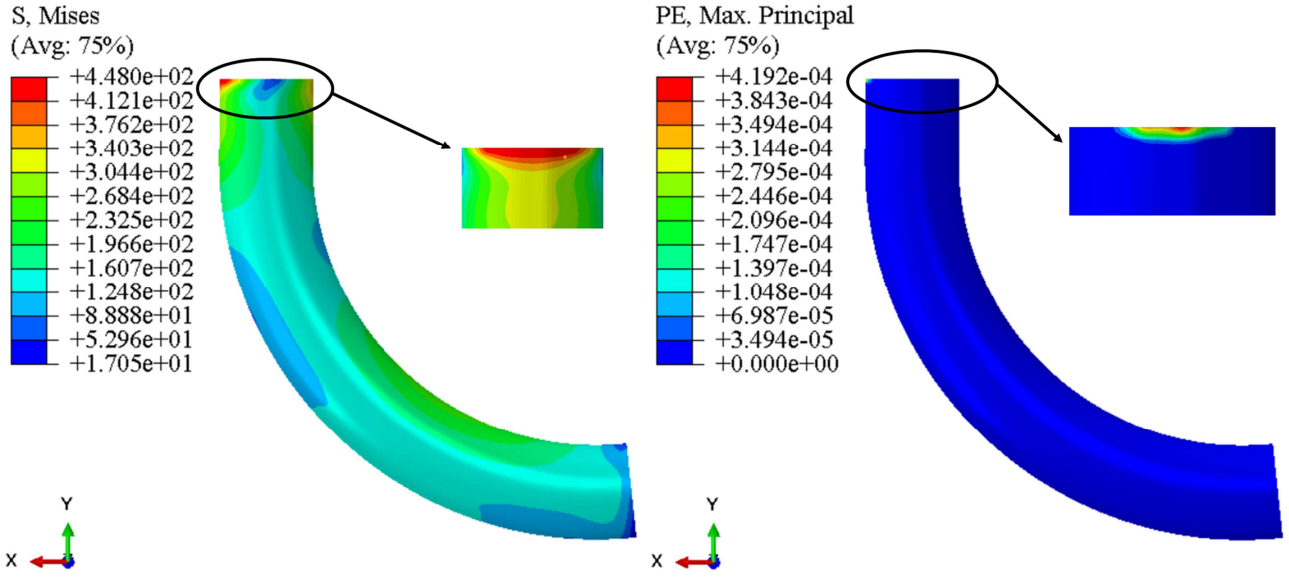

(a) Stress distribution nephogram

(b) End plastic strain

Figure 6. *Cloud chart of pipeline stress and strain distribution.*

Linear eigenvalue buckling analysis is the main method for studying the linear critical loads and modes of submarine pipelines. Linear eigenvalue buckling analysis does not take into account the nonlinearity of the material and the initial defects of the model, such as irregular shape, uneven thickness due to manufacturing errors, and residual stress in the material. Table 6 shows the results of the first five order buckling analysis of submarine pipelines. However, due to the fact that the linear elastic buckling analysis does not consider the initial defects and nonlinearity of the material, the ultimate load obtained at this time is often greater than the true critical load value.

The linear buckling analysis is mainly a linear elastic buckling analysis of the perfect pipe structures without considering the initial geometric defects and material nonlinearity, which leads to large analysis errors. Based on this, this paper introduces the initial defects of circular arc pipes and adds material nonlinearity to further conform to the actual plastic deformation process of pipes. The Riks method in ABAQUS software is used for nonlinear buckling analysis of pipelines, and the initial geometric defects are introduced through the arc length method. Introduce 10% of the pipe

thickness as a defect factor. Figure 7 shows the non-linear buckling load displacement curve of the pipeline.

Table 6. *Fifth order modal and ultimate load of circular arc pipeline.*

Order	1st mode	2nd mode	3rd mode	4th mode	5th mode
$P_{cr\text{-}lin}$ (MPa)	107.72	108.35	110.51	111.61	114.42
Mode	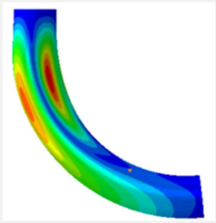	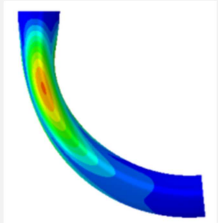	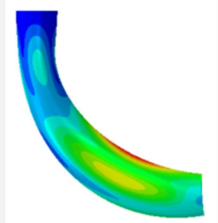	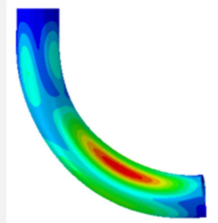	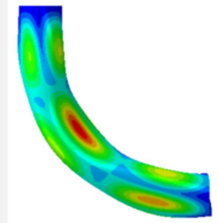

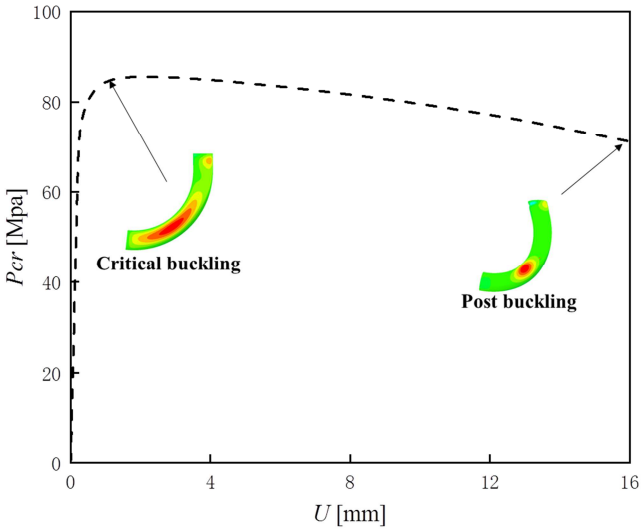

Figure 7. *Pipeline Load Displacement Curve.*

As can be seen from Figure 7, the pipeline undergoes considerable displacement along the X-axis direction when entering post buckling. The position where buckling occurs is at the initial defect. Under critical buckling, overall buckling occurs first, and then local buckling occurs. The load used for the post buckling calculation is 54 MPa, and the critical nonlinear buckling load of the pipe is 85.6 MPa can be derived from Figure 7. Compared with the linear critical buckling load of 107.72 MPa calculated by the first order eigenvalue buckling calculation, it is reduced by 20.5%, indicating that the initial geometric defects have a major impact on the buckling load of the pipe.

5. Conclusion

(1) For pipeline design parameters and manifold arrangement, considering the practical and economic value of manifold design, the design method of deep-sea manifold system is proposed, which can provide reference for the engineering design of deep-water equipment such as underwater pipelines.

(2) The benefits and drawbacks of two ideas for twin wells and dual headers are discussed and evaluated. Lastly, the designed manifold's strength is tested using AutoPIPE software to ensure that it meets the design specifications.

(3) On the curved pipe, linear and nonlinear buckling analyses were done, and the fifth order linear eigenvalue buckling mode, linear critical buckling load, and nonlinear critical buckling load were obtained. The nonlinear buckling critical load was found to be 20.5% lower than the linear critical buckling load, demonstrating that early geometric flaws had a considerable impact on the pipe's bearing capacity.

References

[1] Sang Eui Lee, Jeom Kee Paik, Yeon Chul Ha, et al. An efficient design methodology for subsea manifold piping systems based on parametric studies. Ocean Engineering. 2014, 84 (6): 273-282.

[2] Xu Wenhu, Guo Hong, Hong Yi, et al. Reliability analysis of subsea manifold system and improvement measures. Oil Field Equipment. 2016, 45 (03): 1-6.

[3] Li Qingping, Zhu Haishan, Li Xinzhong, et al. The Current state and future of deep water subsea Production technology. China National Offshore Oil Research Institute. 2016, 18 (02): 76-84.

[4] Wei Yan, Zhang Jinwei, Yu Chenglong, et al. A prospect of domestically manufactured subsea manifold. Shipbuilding of China. 2012, 53 (S2): 153-157.

[5] Chuan Jian, Zhang Guangming, An Weizheng, et al. Research and practice of material localization of deep sea manifolds. China Offshore Platform. 2014, 29 (06): 20-24.

[6] Gu Yongwei, Zhou Meizhen, Wang Changtao, et al. Main structural design and calculation method study of deep water subsea manifold. Mechanical Engineer. 2011. 236 (02): 134-135.

[7] Liu Chao. Research on reliability analysis of subsea oil and gas production system. China, Master thesis. China University of Petroleum (East China), 2020.

[8] Shang Zhaohui, Ruan Weidong, Qiao Hongdong, et al. Study on risk assessment and numerical simulation method of subsea manifold system. Ships and Offshore Structures, 2021, 16 (S1): 245-255.

[9] Wang Yi, Wang Qi, Zhang Aixia, et al. A new optimization algorithm for the layout design of a subsea production system. Ocean Engineering, 2021, 232 (4): 109072.

[10] Liu Chang, Cao Yuguang, Chen Jinzhong, et al. The blockage risk in the elbow of the Bi-directional pig used for submarine pipeline based on the modified Burgers-Frenkel (MB-F) model. Ocean Engineering. 2023, 268: 113508.

[11] Zhang Jingan, Zhuo Wei, Cheng Gangli, et al. Piping System Design of Subsea Manifold. Applied Mechanics and Materials. 2013, 321-324: 1779-1783.

[12] ISO 13628-15: Petroleum and natural gas industries — Design and operation of subsea production systems — Part 15: Subsea structures and manifolds, International organization for standardization: Geneva, Switzerland, 2011.

[13] ASME B31.8: Gas Transmission and Distribution Piping Systems. The American Society of Mechanical Engineers: New York, USA. 2007.

[14] ASME B31.4: Pipeline Transportation Systems for Liquids and Slurries. The American Society of Mechanical Engineers: New York, USA. 1999.

[15] ASME B31.3: Process Piping. The American Society of Mechanical Engineers: New York, USA. 2012.

[16] DNV-RP-F112: Design Of Duplex Stainless Steel Subsea Equipment Exposed To Cathodic Protection. Det Norske Veritas: Oslo, Norway, 2008.

[17] API SPEC 5L. Specification for Line Pipe. American Petroleum Institute: Washington, DC, USA, 2007.

[18] Bai Yong, Bai Qiang, et al. Subsea Engineering Design Manual - Subsea Pipelines Fascicle. Shanghai Jiao Tong University Press: Shanghai, Chain, 2014-8.

[19] Liu Zihe, Guo Zhiyang, Mo Guanggui, et al. Study on buckling of rising section of multilayer marine gas production pipeline. Petrochemical applications. 2021, 40 (08): 32-37.